Probing the Role of Parasite-Specific, Distant Structural Regions on Communication and Catalysis in the Bifunctional Thymidylate Synthase−Dihydrofolate Reductase from *Plasmodium falciparum*†

Tina Dasgupta and Karen S. Anderson*

Department of Pharmacology, Yale University School of Medicine, 333 Cedar Street, New Haven, Connecticut 06511

Received August 10, 2007; Revised Manuscript Received November 15, 2007

ABSTRACT: *Plasmodium falciparum* thymidylate synthase−dihydrofolate reductase (TS-DHFR) is an essential enzyme in nucleotide biosynthesis and a validated molecular drug target in malaria. Because *P. falciparum* TS and DHFR are highly homologous to their human counterparts, existing active-site antifolate drugs can have dose-limiting toxicities. In humans, TS and DHFR are two separate proteins. In *P. falciparum*, however, TS-DHFR is bifunctional, with both TS and DHFR active sites on a single polypeptide chain of the enzyme. Consequently, *P. falciparum* TS-DHFR contains unique distant or nonactive regions that might modulate catalysis: (1) an N-terminal tail and (2) a linker region tethering DHFR to TS, and encoding a crossover helix that forms critical electrostatic interactions with the DHFR active site. The role of these nonactive sites in the bifunctional *P. falciparum* TS-DHFR is unknown. We report the first in-depth, pre-steady-state kinetic characterization of the full-length, wild-type (WT) *P. falciparum* TS-DHFR enzyme and probe the role of distant, nonactive regions through mutational analysis. We show that the overall rate-limiting step in the WT *P. falciparum* TS-DHFR enzyme is TS catalysis. We further show that if TS is in an activated (liganded) conformation, the DHFR rate is 2-fold activated, from 60 s^{-1} to 130 s^{-1} in the WT enzyme. The TS rate is also reciprocally activated by ∼1.5-fold if DHFR is in an activated, ligand-bound conformation. Mutations to the linker region affect neither catalytic rate nor domain−domain communication. Deletion of the N-terminal tail, although in a location remote from the active site, decreases the DHFR single rate and the bifunctional TS-DHFR rate by a factor of 2. The 2-fold activation of the DHFR rate by TS ligands remains intact, although even the activated N-terminal mutant has just half the DHFR activity of the WT enzyme. However, the reciprocal communication between TS active site and DHFR ligands is impaired in N-terminal mutants. Surprisingly, deletion of the analogous N-terminal tail in *Leishmania major* TS-DHFR causes a 3-fold *enhancement* of the DHFR rate from ∼14 s^{-1} to ∼40 s^{-1}. In summary, our results demonstrate a complex interplay of domain−domain communication and nonactive-site modulation of catalysis in *P. falciparum* TS-DHFR. Furthermore, each parasitic TS-DHFR is activated by unique mechanisms, modulated by their nonactive site regions. Finally, our studies suggest the N-terminal tail of *P. falciparum* TS-DHFR is a highly selective, novel target for potential antifolate development in malaria.

Malaria is a parasitic disease that kills over 3000 people per day and infects some 300 million people per year. The causative agents of malaria are *Plasmodium* spp. parasites, bred in warm stagnant waters and spread in humans by the bite of the *Anopheles* mosquito. While many species of *Plasmodium* are endemic to different regions, it is *Plasmodium falciparum* that accounts for over 90% of malaria-related deaths. Despite advances in health care, mortality from malaria has increased by nearly 25% over the past decade in sub-Saharan Africa, due in large part to an increase in drug-resistant parasites. High-dose therapy is often limited by the toxicity of the antimalarial drugs (*1*). New, targeted therapies are urgently needed.

Thymidylate synthase−dihydrofolate reductase (TS-DHFR)[1] is a critical metabolic enzyme and validated drug target in *P. falciparum* (*2*). As illustrated in Figure 1a, TS catalyzes the conversion of methylenetetrahydrofolate (CH_2H_4-folate) to dihydrofolate (H_2folate) while methylating 2′-deoxyuridine monophosphate (dUMP) to 2′-thymidine monophosphate (dTMP) (*2*). DHFR subsequently converts H_2folate to H_4folate while oxidizing NADPH to $NADP^+$. Both H_2- and H_4folate are important metabolites in the nucleotide biosynthesis pathway; consequently, active-site inhibitors of

† This work was supported in part by NIH Grant AI 44630 (to K.S.A.), by an NIH Medical Student Training Program grant to the Yale M.D.−Ph.D. Program (to T.D.), and by a doctoral research award from the Canadian Institutes of Health Research (to T.D.).

* Corresponding author: tel (203) 785-4526; fax (203) 785-7670; e-mail karen.anderson@yale.edu.

[1] Abbreviations: TS-DHFR, thymidylate synthase−dihydrofolate reductase (this is a functional designation, as dihydrofolate is produced at TS and utilized at DHFR; this enzyme is also commonly referred to as DHFR-TS in the literature because the DHFR domain is N-terminal to the TS domain); dUMP, deoxyuridine monophosphate; dTMP, thymidine monophosphate; CH_2H_4folate, methylenetetrahydrofolate; H_2-folate, dihydrofolate; H_4folate, tetrahydrofolate; NADPH, nicotinamide adenine dinucleotide phosphate; HPLC, high-performance liquid chromatography.

10.1021/bi701624u CCC: $40.75
Published on Web 01/12/2008

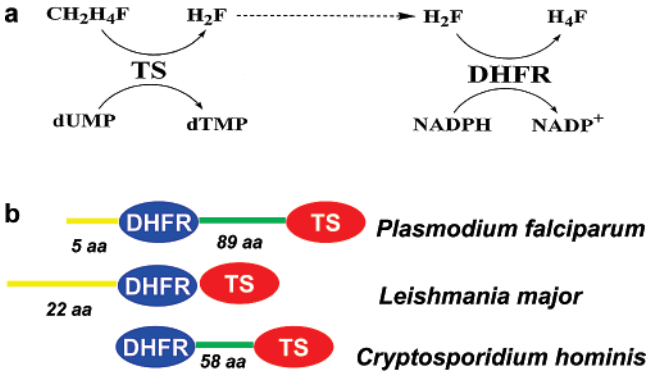

FIGURE 1: Reaction scheme and the nonactive-site regions of bifunctional parasitic TS-DHFR enzymes. (a) TS catalyzes the conversion of CH_2H_4folate and dUMP to dTMP and H_2folate. H_2-Folate is converted to H_4folate at the DHFR active site while an NADPH is oxidized to $NADP^+$. (b) Diagrammatic representation of organism-specific differences in nonactive-site regions of TS-DHFR. The N-terminal tail (yellow) of the DHFR active site (blue) can be of variable length or completely absent. This is also true of the linker or junctional region (green), which links the DHFR and TS (red) active sites.

P. falciparum DHFR (e.g., pyrimethamine, cycloguanil) have been used successfully in antifolate therapy in malaria (*3*).

TS-DHFR is a bifunctional enzyme. Most higher eukaryotes, including humans and prokaryotes, express TS and DHFR as two discrete enzymes. However, several human parasites like *P. falciparum* encode TS and DHFR on a single polypeptide chain, with DHFR N-terminal to TS (*2*−*4*). Previous studies have highlighted novel characteristics of these bifunctional enzymes, with significant variation in different parasites (*5*−*7*). One such interesting property is domain−domain communication: if the TS active site is liganded in the *Leishmania major* TS-DHFR, a 10-fold activation of the DHFR rate results (*6*). Conformational changes in TS and DHFR are thought to modulate this domain−domain communication (*4*). Notably, this activation is absent in the *Cryptosporidium hominis* enzyme (*5*) and has not previously been explored in *P. falciparum* TS-DHFR.

Because TS and DHFR are evolutionarily well-conserved, there is high homology with the corresponding enzymes from other eukaryotes (including humans). However, flanking the TS and DHFR active sites in parasitic TS-DHFRs are distinct, distant structural or "nonactive-site" regions, which have no homology between organisms (*8*−*10*). Our work thus focuses on two such nonactive-site regions in *P. falciparum* TS-DHFR: the crossover helix of the linker region and the N-terminal tail (Figure 1b).

The linker, a long region connecting TS and DHFR, is 89 and 52 amino acids (aa) in *P. falciparum* and *C. hominis*, respectively. The *L. major* TS-DHFR has no linker (Figure 1b). Although there is no sequence homology between the linkers of *P. falciparum* and *C. hominis*, both encode a 15-aa crossover helix, one face of which forms electrostatic interactions with the backside of the DHFR active site (*8*−*10*). The crossover helices in *C. hominis* and *P. falciparum* TS-DHFR vary in their amino acid compositions and interactions. In *C. hominis*, the face of the crossover is composed of hydrophilic and hydrophobic residues (like S195, D198, L202, I206, and R210), which interact with several important residues in the DHFR backbone (like Y132, N42, F35, F172, and E31). However, remarkably, the crossover helix in *P. falciparum* TS-DHFR (residues 283−295) has numerous acidic residues (residues 283−289 are either Asp or Glu, followed by F290, V291, Y292, F293, N294, and F295), which form electrostatic interactions with the many positively charged residues (primarily Lys) in the backside of the DHFR active site (shown in Figure 2b). Mutational disruption of the electrostatic interactions of the crossover helix in *C. hominis* TS-DHFR diminishes DHFR catalytic rates by 10-fold if the entire crossover helix is substituted with alanines or by 3-fold with alanine substitution of only the face of the helix that forms interactions with the DHFR active site (*11*). However, the kinetic consequences of disrupting the electrostatic interactions crossover helix in *P. falciparum* TS-DHFR have not yet been studied. The interactions between the crossover helix face and the DHFR active site that can potentially be disrupted by mutagenesis are shown in Figure 2b.

The N-terminal tail comprises the first few amino acids preceding the DHFR domains in certain TS-DHFRs. *P. falciparum* TS-DHFR has a 6 aa long N-terminal tail, oriented away from the DHFR, in a position remote from the active site (*9*) (Figure 2a,c). The N-terminal tail is absent in *C. hominis* TS-DHFR; in *L. major*, it is 22 aa long and is of unknown function (Figure 1b). The *L. major* N-terminal tail has no homology to its counterpart in *P. falciparum*; it wraps around the surface of the bifunctional enzyme, making extensive direct contacts with the TS domain (*10*). Studies done on the monofunctional *P. falciparum* DHFR and TS enzymes suggest that deletions of the N-terminal region decrease activity of DHFR and coexpressed TS (*12*, *13*). However, the role of the N-terminal tail in modulating catalysis in the full-length, bifunctional TS-DHFR enzyme has not yet been studied.

To investigate the kinetics of the WT *P. falciparum* TS-DHFR and the role of its nonactive-site regions, we used pre-steady-state kinetic analysis. Transient kinetic methodology allows one to follow chemical catalysis individually at both TS and DHFR active sites, to investigate chemical rates of all three reactions (TS, DHFR, and TS-DHFR) individually, to monitor intermediates as they shift from one active site to another, and to investigate the importance of communication between these active sites.

Our first objective was a detailed transient kinetic analysis of the wild-type (WT) *P. falciparum* TS-DHFR enzyme. Specifically, using rapid chemical quench and stopped-flow fluorescence, we asked whether communication occurs between the TS and DHFR domains of the enzyme. Our second objective was to determine whether the electrostatic interactions of the crossover helix play an important role in catalysis and communication in *P. falciparum* TS-DHFR. The face of the crossover helix that interacts with the DHFR active site is comprised of five residues; we substituted only these five residues with alanines to form the Ala-FACE helix mutant, or we replaced the entire crossover helix with alanines to form the all-Ala helix mutant of *P. falciparum* TS-DHFR. Finally, our third objective was to understand the effects of an N-terminal tail mutation on the pre-steady-state kinetics of the bifunctional, full-length *P. falciparum* TS-DHFR enzyme. The results of deleting residues 2−5 of N-terminal tail in *P. falciparum* (mutant D4) were compared to those of an analogous deletion of residues 2−22 of the N-terminal tail in *L. major* (mutant N22). We used the same

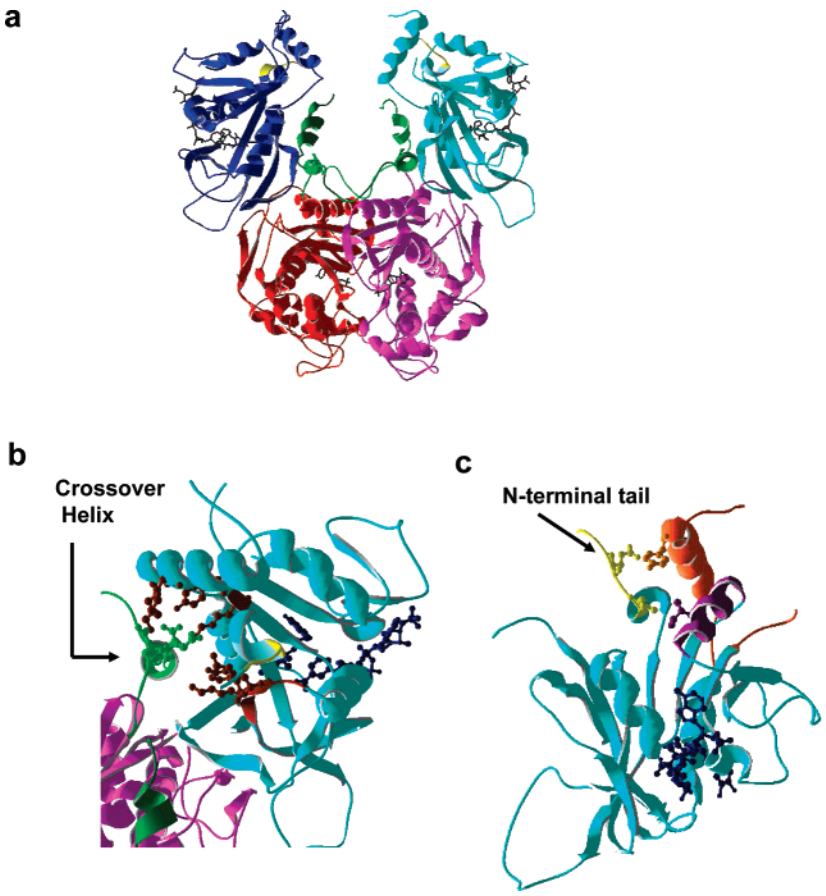

FIGURE 2: Nonactive-site regions of *P. falciparum* TS-DHFR enzymes, highlighting the interactions disrupted in the Ala-FACE and D4 mutants. (a) The *P. falciparum* TS-DHFR structure (PDB entry 1J3I) is colored with DHFR domains in blue and TS in red, with the linker region highlighted in green and the N-terminal tail in yellow. (b) Interactions between the crossover helix (green) and the backside DHFR active site (burgundy) disrupted by the Ala-FACE mutant. The residues shown are Asp 284, Glu 285, Asp 288, Asp 289, and Tyr 292 in the crossover helix and Lys 69, Lys 72, Tyr 158, Lys 160, Lys 180, Lys 181, and Tyr 183 in the DHFR backbone. Substrates WR99210 and NADPH are shown in navy blue to mark the active site. For clarity, only a single DHFR monomer and its adjacent TS domain are shown, and also the residues Asn 231 to Asp 222 and Lys 227 are not shown. (c) Interactions of the residues of the N-terminal tail (shown in yellow) with insert II (shown in orange) and with the αE−βE loop (shown in purple). The residues highlighted are Glu 3 and Val 5 in the N-terminal tail, Tyr 90 in insert II, and Ile 50 in the αE−βE loop. The substrates WR99210 (*23*) and NADPH are shown in navy blue to mark the active site. Only a single DHFR domain is shown for clarity.

nomenclature for the *P. falciparum* N-terminal mutants as described previously in the literature (*12*).

This is the first systematic, transient kinetic characterization of the WT *P.* falciparum TS-DHFR enzyme and of the nonactive-site regions of any bifunctional parasitic TS-DHFR. We demonstrate that elegant communication exists between the TS and DHFR active sites of *P. falciparum* TS-DHFR. Also, we show that mutations of the linker crossover helix do not disrupt the catalytic rates in this enzyme. A 4 aa deletion of the N-terminal tail, however, affects the chemical rates of the TS, DHFR, and TS-DHFR reactions in *P. falciparum* TS-DHFR. Surprisingly, analogous mutations in the *L. major* N-terminal tail increase the DHFR chemical rate of the enzyme, suggesting differential regulation between bifunctional TS-DHFRs from different organisms. Our studies of the *P. falciparum* TS-DHFR enzyme highlight the unique regulation of the kinetic mechanisms of bifunctional parasitic TS-DHFR enzymes, especially since *P. falciparum* encodes both an N-terminal tail and a linker with crossover helix. Since TS-DHFR is also a validated drug target, understanding the role of these distinct structural regions may also aid in rational drug design for the development of more targeted and less toxic therapies for this deadly disease.

MATERIALS AND METHODS

Reagents, Chemicals, and Bacterial Strains. We used reagents of the highest available commercial grade. Millipore ultrapure water was used in the preparation of all solutions. β-Nicotinamine adenine dinucleotide 2′-phosphate (NADPH), 2′-deoxyuridine 5′-monophosphate disodium salt (dUMP), 5-fluoro-2′-deoxyuridine 5′-monophosphate sodium salt (FdUMP), sodium hydrosulfite, chloramphenicol, and methotrexate agarose were purchased from Sigma−Aldrich (St Louis, MO). 1,4-Dithitothreitol, isopropyl β-D-thiogalactopyranoside (IPTG) and ampicillin (D-α-aminobenzylpenicillin) were purchased from American Bioanalytical. Luria broth (LB) and Terrific broth (TB) were obtained from Invitrogen (Carlsbad, Ca) and VWR International (West Chester, PA), respectively.

The tritiated H_2folate was prepared also by reducing commercially available [3′,5′,7,9-$^3H_4$]folic acid (Moravek Biochemicals, Brea, CA) with sodium hydrosulfite and purified by use of a triethylammonium bicarbonate (TEAB)

gradient on DE-52 resin (*14*, *15*). CH_2H_4folate (methylenetetrahydrofolate) was prepared first by enzymatic conversion of H_2folate to (6*R*,*S*)-5,6,7,8-tetrahydrofolate and then by a condensation reaction in the presence of formaldehyde. Radiolabeled CH_2H_4folate was prepared from tritiated H_2folate, with the synthesis otherwise identical to that of the unlabeled CH_2H_4folate. Both unlabeled and tritiated CH_2H_4folate were purified by use of a TEAB gradient on DE-52 resin (Whatman) (*14*, *15*). The purity of the radiolabeled substrates was confirmed by HPLC analysis (see below). Calcium-competent *Escherichia coli* strain BL21 (DE3) pLysS was purchased from Invitrogen (Carlsbad, CA).

Enzyme Mutagenesis, Expression, and Purification. The plasmid expressing the TM4/8.2 strain of wild-type *P. falciparum* TS-DHFR is a generous gift from Drs. Penchit Chitnumsub and Yongyuth Yuthavong (BIOTEC, National Science and Technology Development Agency, Thailand) (*16*). Using the QuikChange site-directed mutagenesis kit (Stratagene, La Jolla, CA), we mutated *P. falciparum* TS-DHFR residues 283−295 to Ala to create an all-alanine crossover helix, and we mutated residues 284, 285, 288, 289, and 292 to Ala to make the Ala-FACE crossover helix. We also deleted residues 2−5 to make the N-terminal tail mutant D4 and residues 2−6 to make the mutant D5. Primers were synthesized and gel-purified by the Yale Keck Facility according to protocols available online. The mutated plasmids were amplified in calcium-competent DH5α *Escherichia coli* cells and then purified by use of the Qiaprep spin miniprep kit (Qiagen, Valencia, CA). Plasmids were sequenced by the Yale Keck Facility (New Haven, CT) to confirm the mutagenesis and were stored at −20 °C. Concentration of DNA was determined spectrophotometrically by absorbance at 260 nm. The plasmid expressing the TS-DHFR enzyme from *L. major* was the generous gift of C.-C. Kan and D. Matthews (Agouron Pharmaceuticals, La Jolla, CA). Its N-terminal residues 2−22 were deleted by use of QuikChange (Stratagene, La Jolla, CA) to create the N-terminal mutant N22. The plasmid was cloned into a pET11b for expression in *E. coli* BL21 cells. All plasmids were sequenced by the Yale Keck Facility to confirm mutagenesis.

The *P. falciparum* WT TS-DHFR was expressed and purified as previously described (*16*). The protocol for expression of Ala-FACE and all-Ala helix mutants was identical to that for wild-type *P. falciparum* TS-DHFR. The protocols for expression and purification of the D4 and D5 N-terminal mutants were also identical to that for the WT enzyme, except that 350 mM KCl (instead of 1 M KCl) was used to wash the unbound enzyme off the methotrexate affinity resin. The active-site concentrations of WT and mutant enzymes were equivalent, as determined by pre-steady-state burst amplitudes of their DHFR reactions (see below). The methods for expression and purification of *L. major* TS-DHFR WT and N23 deletion mutant were as described previously (*6*).

Assessment of Enzyme Concentration and Activity. Enzyme concentration was determined spectrophotometrically by following absorbance at 280 nm. The extinction coefficient for *P. falciparum* TS-DHFR is 83 740 M^{-1} cm^{-1} and for *L. major* TS-DHFR is 69 955 M^{-1} cm^{-1}. DHFR steady-state activity was assessed by reacting enzyme with H_2folate and NADPH and following absorbance at 340 nm, which decreases as NADPH is depleted to form $NADP^+$. An extinction coefficient of -12.8 mM^{-1} cm^{-1} was used for the DHFR reaction. TS-DHFR steady-state activity was assayed by incubating the enzyme with CH_2H_4folate, NADPH, and dUMP, and following the increase in absorbance at 340 nm with the production of dTMP and H4-folate. An extinction coefficient of -6.4 mM^{-1} cm^{-1} was used for the TS reaction (*17*).

Rapid Chemical Quench Experiments. We performed rapid chemical quench experiments on a Kintek RFQ-3 rapid chemical quench apparatus (Kintek Instruments, Austin, TX) to enable us to study enzymatic experiments on a millisecond time scale. All reactions were performed at 25 °C. The reactions involved mixing 15 μL of enzyme solution with 15 μL of substrate solution. The substrates were tritiated (as described above), which enabled subsequent high-performance liquid chromatographic (HPLC) analysis to follow the reaction substrates and products (see below for details). The enzyme solution consisted of a mixture of enzyme, nonlimiting substrate, and 2× reaction buffer (50 mM $MgCl_2$, 1 mM EDTA, and 50 mM Tris-HCl, pH 7.8). The substrate solution consisted of approximately 20 000 dpm of the appropriate tritiated substrate. The DHFR single-turnover experiment consisted of mixing an enzyme solution of enzyme, NADPH, and 2× reaction buffer with a substrate solution of tritiated H_2folate. The TS single-turnover experiment consisted of mixing an enzyme solution of enzyme, dUMP, and 2× reaction buffer with a substrate solution of tritiated CH_2H_4folate. Finally, the TS-DHFR bifunctional single-turnover experiment consisted of mixing an enzyme solution of enzyme, dUMP, NADPH and 2× reaction buffer with a substrate solution of tritiated CH_2H_4folate. All reactions were quenched by addition of 67 μL of 0.78 M KOH solution. In each reaction, the final concentration of reaction buffer was 1×. All concentrations for enzyme and substrate listed in the text are final concentrations after mixing.

High-Performance Liquid Chromatographic Analysis. The tritiated reaction products from the rapid chemical quench reactions were analyzed by HPLC with radioactivity and ultraviolet flow detectors. A BDS-Hypersil C18 reverse-phase column (250 × 4.6 mm^2, Keystone Scientific, Bellefonte, PA) was used for separation. We used a solvent consisting of 10% methanol in 180 mM triethylammonium bicarbonate (pH 7.8), in isocratic separation mode at a flow rate of 1 mL/min, for optimal separation of our substrates and products. Under these conditions, tritiated H_4folate eluted at 7 min, tritiated H_2folate at 14 min, and tritiated CH_2H_4folate at 15 min.

Stopped-Flow Experiments. We used a Kintek SF-2001 stopped-flow apparatus (Kintek Instruments, Austin, TX) to probe communication between the TS and DHFR domains. Reactions were performed under burst conditions, in which substrate concentration is in slight excess over enzyme concentration. For the DHFR reaction, the enzyme solution, consisting of enzyme, NADPH, ±CH_2H_4folate, ±FdUMP, and 2× reaction buffer, was mixed with the substrate solution of H_2folate. For the TS reaction, the enzyme solution, consisting of enzyme and dUMP ±NADPH, was mixed with the substrate solution of CH_2H_4folate. For the DHFR reaction, we excited the reaction at 287 nm and followed the fluorescent resonance energy transfer (FRET) at 450 nm. For the TS reaction, we excited the reaction at 287 nm and followed the fluorescent emission at 340 nm.

RESULTS

Expression of P. falciparum WT and Mutant TS-DHFR Enzymes. We were able to produce 0.28 mg of WT enzyme, 0.29 mg of Ala-FACE enzyme, and 0.14 mg of D4 pure protein per liter of *E. coli* culture. The DHFR steady-state rates for the WT, Ala-FACE, and D4 enzymes were 16.7 ± 0.164 s^{-1}, 17.6 ± 0.258 s^{-1}, and 0.496 ± 0.00421 s^{-1}, respectively. The bifunctional TS-DHFR steady-state rates for the WT, Ala-FACE, and D4 enzymes were 1.77 ± 0.0795 s^{-1}, 1.875 ± 0.0693 s^{-1}, and 2.53 ± (0.537 × 10^{-2}) s^{-1}, respectively. We also mutated the *P. falciparum* TS-DHFR plasmid to encode an all-Ala crossover helix. The full-length, all-Ala enzyme consistently copurified with a 39 kDa band, which was confirmed by mass spectrometry to be a fragment of *P. falciparum* TS-DHFR (and not an *E. coli* TS or DHFR enzyme). Despite the use of high concentrations of protease inhibitors and expedited protein purification, degradation of the all-Ala mutant into this 39 kDa fragment could not be prevented. Under these conditions, only 0.01 mg of pure all-Ala helix mutant could be expressed per liter of *E. coli* culture. When we tried to express a mutant with the crossover helix completely deleted, the protein was consistently degraded intracellularly. The interactions disrupted by the Ala-FACE and N-terminal deletion mutants are highlighted in Figure 2b,c.

We also tried to express the D5 mutant of the N-terminal tail in which residues 2−6 of *P. falciparum* WT TS-DHFR were deleted. Protein expression was too low to allow a detailed kinetic characterization of the protein; however, the expressed enzyme reproducibly showed DHFR activity by spectrophotometric analysis.

Single-Turnover Experiments for DHFR Reaction for P. falciparum TS-DHFR. To examine the DHFR activity for WT and for Ala-FACE, and D4 mutants, single enzyme turnover experiments were conducted by a rapid chemical quench approach. The formation of tritiated H_4folate was monitored over time by HPLC analysis of the reaction products. We preincubated 80 μM of the appropriate enzyme and a saturating concentration of NADPH (500 μM) and then added 6.5 μM tritiated H_2folate. All reactions were carried out to completion but only the earlier time points are shown here for clarity (Figure 3a). The data were fit to a single-exponential equation, and the rate constants for WT and the Ala-FACE mutant were similar at 80 ± 5.2 s^{-1} and 64 ± 4.4 s^{-1}, respectively. The rate constant for the D4 mutant was ~2-fold slower than WT at 38 ± 2.4 s^{-1}.

Single-Turnover Experiments for the TS Reaction for P. falciparum TS-DHFR. To examine the TS activity for WT and for Ala-FACE and D4 mutants, single enzyme turnover experiments were conducted, again by a rapid chemical quench approach. The formation of tritiated H_2folate was followed over time by HPLC analysis of the reaction products. In these experiments, 80 μM of the appropriate enzyme was preincubated with a saturating concentration of dUMP (500 μM) and then mixed with 6.5 μM tritiated CH_2H_4folate. All reactions were carried out to completion but only a subset of the data is shown here (Figure 3b). The data were fit to a single-exponential equation, and the rate constants for WT and the Ala-FACE mutant were similar at 1.2 ± 0.22 s^{-1} and 1.4 ± 0.28 s^{-1}, respectively. The rate constant for the D4 N-terminal tail mutant was 0.84 ± 0.083 s^{-1}, demonstrating that the TS activity of the enzyme for the D4 is very similar to that of the WT enzyme. These results are summarized in Table 1.

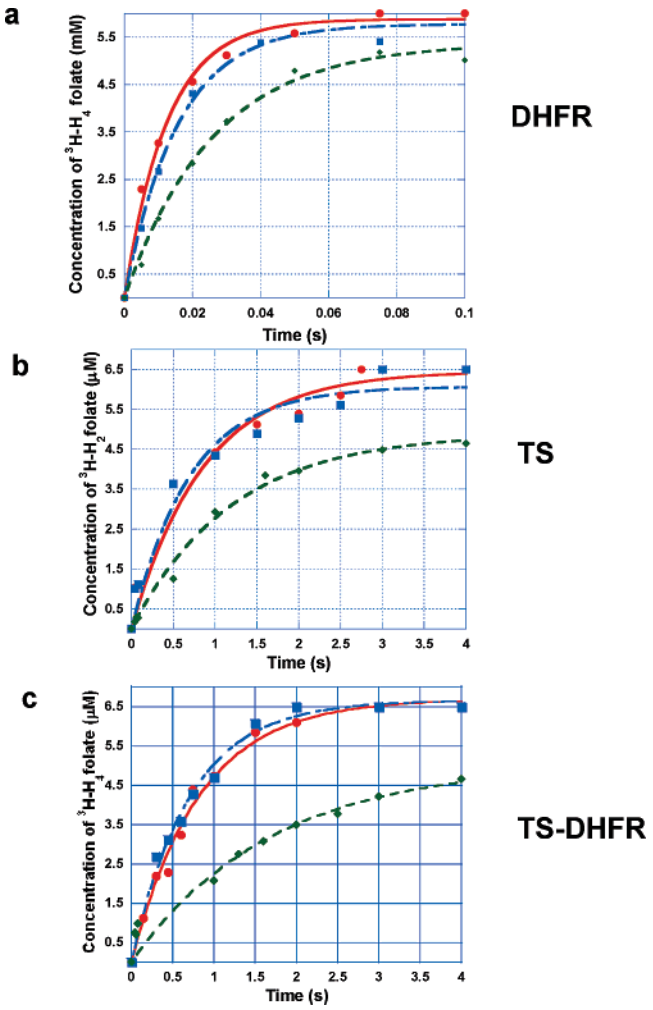

FIGURE 3: Single-turnover experiments for WT and for Ala-FACE and D4 mutants of *P. falciparum* TS-DHFR show the N-terminal tail mutant slows all three reactions: TS, DHFR, and TS-DHFR. Data for WT enzyme (red circles), Ala-FACE mutant (blue squares), and D4 N-terminal mutant (green diamondd) are plotted for each reaction. The reactions were conducted in a rapid chemical quench apparatus under single-turnover conditions at 25 °C. (a) The DHFR experiment was conducted with 80 μM enzyme and 500 μM NADPH mixed with 6.5 μM tritiated H_2folate. (b) The TS experiment was conducted with 80 μM enzyme and 500 μM dUMP mixed with 6.5 μM tritiated CH_2H_4folate. (c) The bifunctional TS-DHFR experiment was conducted with 80 μM enzyme, 500 μM NADPH, and 500 μM dUMP mixed with 6.5 μM tritiated CH_2H_4folate. In all cases, the data were fit to a single-exponential equation, and the rate constants from these are summarized in Table 1.

Single-Turnover Experiments for the Bifunctional Reaction for P. falciparum TS-DHFR. To examine the TS-DHFR bifunctional activity for WT and for Ala-FACE and D4 mutants, single enzyme turnover experiments were conducted with a similar rapid chemical quench approach. In this case, the formation of tritiated H_4folate was monitored over time by HPLC analysis of the reaction products. We preincubated 80 μM of the appropriate enzyme with a saturating concentration of dUMP (500 μM) and NADPH (500 μM) and then added 6.5 μM tritiated CH_2H_4folate. The reactions were carried out to completion but only a subset of the data is shown here for clarity (Figure 3c). The data were fit to a

Table 1: Summary of Single Turnover Results from Rapid Chemical Quench Experiments[a]

enzyme	DHFR rate constant (s^{-1})	TS rate constant (s^{-1})	bifunctional TS-DHFR rate constant (s^{-1})
WT	80 ± 5.2	1.2 ± 0.22	1.2 ± 0.085
Ala-FACE	64 ± 4.4	1.4 ± 0.28	1.4 ± 0.091
D4	38 ± 2.4	0.84 ± 0.083	0.60 ± 0.15

[a] The data were fit to a single-exponential equation, and the conditions used were as summarized in the legend for Figure 3.

single-exponential equation, and the rate constants for WT and the Ala-FACE mutant were similar at 1.2 ± 0.085 s^{-1} and 1.4 ± 0.091 s^{-1}, respectively. The rate constant for the D4 N-terminal tail mutant for this same reaction is only half that, at 0.60 ± 0.15 s^{-1}. These results are summarized in Figure 3c and Table 1.

Pre-Steady-State Burst Experiments of the DHFR Reaction for P. falciparum TS-DHFR. NADPH bound to the DHFR active site produces a fluorescent resonant energy transfer (FRET) at 450 nm. As H_2folate is added, the NADPH bound at the active site is oxidized to $NADP^+$, producing a decrease in fluorescence. Thus, stopped-flow fluorescence studies can be used to follow consumption of NADPH at the DHFR active site on a millisecond time scale. The purpose of these particular studies was to confirm the rapid chemical quench DHFR chemical rates determined by following the production of H_4folate. In these reactions, the corresponding enzyme (7.5 μM) was preincubated with 500 μM NADPH, and then 50 μM H_2folate was added in the stopped-flow apparatus. Excitation was at 287 nm and emission was at 450 nm. The data were fit to a single-exponential burst equation (Figure 4 a), and the rate constants are reported in Table 2. The chemical rates determined from the stopped-flow burst experiments are very similar to those obtained by rapid chemical quench single-turnover experiments. Importantly, these results also confirm that the D4 mutant has a DHFR rate constant about half that of the WT and Ala-FACE enzymes.

DHFR Activation Reaction in the Presence of TS Ligands FdUMP and CH_2H_4Folate. We also monitored DHFR activity in the presence of the two TS ligands, CH_2H_4folate and FdUMP (a dead-end inhibitor of TS), for WT and mutant *P. falciparum* TS-DHFRs. The corresponding enzyme (7.5 μM) was preincubated with 500 μM NADPH, 100 μM FdUMP, and 25 μM CH_2H_4folate, and then 50 μM H_2folate was added in the stopped-flow apparatus. Excitation was at 287 nm and emission was at 450 nm. The data were fit to a single-exponential burst equation (Figure 4b) and summarized in Table 2. In the presence of TS ligands, the chemical rate is almost doubled in all three enzymes—WT, Ala-FACE, and D4—and the D4 rate remains about half that of the WT enzyme.

Pre-Steady-State Burst Experiments of the TS Reaction in the Absence and Presence of the DHFR Ligand NADPH. We also asked the reciprocal question of whether the TS rate is activated by the DHFR ligand NADPH. Using the stopped-flow apparatus, we followed the change in intrinsic fluorescence at the TS active site upon substrate binding and conversion to product. Excitation was at 287 nm and emission was at 340 nm. We preincubated the corresponding enzyme (7.5 μM) with 100 μM dUMP and mixed this with 25 μM CH_2H_4folate. For the experiment in the presence of NADPH, the corresponding enzyme (7.5 μM) was preincubated with 100 μM dUMP and 500 μM NADPH, and then 25 μM CH_2H_4folate was added in the stopped-flow apparatus. The data were fit to a single-exponential burst equation. The TS rates, in the absence of DHFR ligand NADPH, for WT and for Ala-FACE and D4 mutants were 9.94 ± 0.203 s^{-1}, 8.58 ± 0.249 s^{-1}, and 10.1 ± 0.507 s^{-1}, respectively. However, the TS rates in the presence of NADPH were 15.3 ± 0.428 s^{-1}, 13.2 ± 0.324 s^{-1}, and 10.3 ± 0.541 s^{-1}, respectively. Thus, the DHFR ligand NADPH seems to activate the TS burst rate in WT and Ala-FACE enzymes but not in the D4 mutant.

L. major N22 DHFR Single-Turnover and Pre-Steady-State DHFR Burst. We also expressed the *L. major* WT bifunctional TS-DHFR enzyme and a mutation in which only its N-terminal tail is deleted (N22). Though expression of N22 was about 0.07 mg of pure protein/L of *E. coli* culture, DHFR single-turnover and pre-steady-state burst experiments could be performed. As described above, 45 μM *L. major* WT or N22 TS-DHFR was preincubated with 500 μM NADPH, and then 5.5 μM tritiated H_2folate was added in the rapid chemical quench apparatus. The production of tritiated H_4folate was monitored over time by HPLC analysis. The rate constant for DHFR is 40.2 ± 4.60 s^{-1} in the N22 mutant (Figure 5a), compared to the WT *L. major* DHFR catalytic rate of 14.5 ± 1.37 s^{-1} (data not shown). The DHFR rate constant for the WT *L. major* enzyme is similar to previously published data (*6*). However, the fast chemical rate was unexpected in the N22 mutant. To confirm this fast rate, a pre-steady-state DHFR burst experiment of the N22 enzyme was also performed by stopped-flow analysis, as outlined above for the *P. falciparum* enzyme. We preincubated 7.5 μM enzyme and 500 μM NADPH and then added 50 μM H_2folate. Excitation was at 287 nm and emission was at 450 nm, and the data were fit to a single exponential. The DHFR burst rate constant for the N22 mutant was 45.21 ± 0.853 s^{-1} (Figure 5b), which is in good agreement with our single-turnover rate.

DISCUSSION

Kinetics of the Wild-Tpe P. falciparum TS-DHFR Enzyme. This is the first report of the single-turnover rate constants for the TS, DHFR, and bifunctional TS-DHFR reactions for *P. falciparum* TS-DHFR. We have shown that, in WT *P. falciparum* TS-DHFR, the DHFR chemical rate (70 s^{-1}) is significantly faster than TS. TS is the rate-limiting step in both the TS reaction and the bifunctional TS-DHFR reaction with a chemical rate of ~1 s^{-1} (Table 1), an observation consistent with the known kinetic mechanisms for other parasitic TS-DHFRs (*5*, *6*).

This is also the first report of domain−domain communication in *P. falciparum* TS-DHFR. We show that if the TS active site is liganded in the *P. falciparum* TS-DHFR, the DHFR chemical rate is nearly doubled to ~130 s^{-1} (Table 2). This communication between TS and DHFR active sites is important for three reasons. First, the activation of *P. falciparum* DHFR is analogous to the regulation of DHFR activity in the *L. major* TS-DHFR enzyme but very different from that of *C. hominis* and *Toxoplasma gondii* TS-DHFRs, which are activated regardless of whether ligands are bound

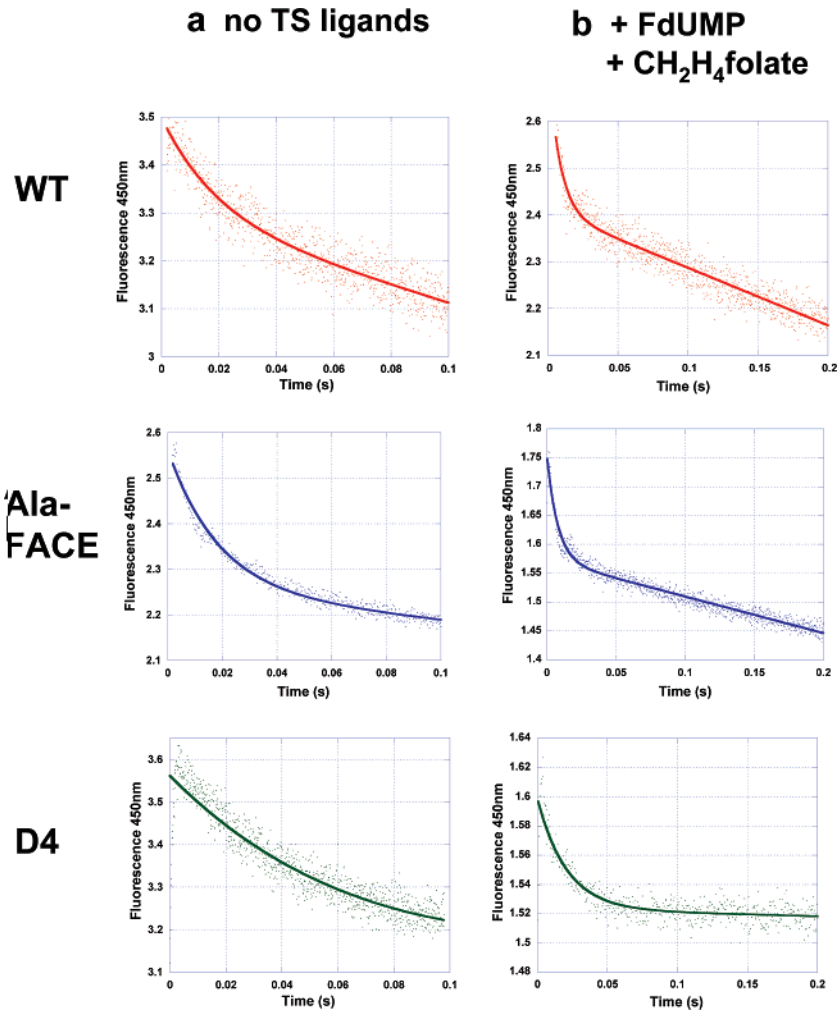

FIGURE 4: DHFR rate in *P. falciparum* TS-DHFR is activated in the presence of TS ligands dUMP and CH_2H_4folate. DHFR burst experiments for WT and for Ala-FACE and D4 N-terminal mutants were conducted in the presence or absence of TS ligands. Using stopped-flow fluorescence, we performed these experiments under burst conditions, with fluorescence excitation at 287 nm and the emission at 450 nm. Column a shows data from DHFR burst experiments conducted in the absence of TS ligands. The conditions were used were 7.5 μM enzyme and 500 μM NADPH, mixed with 50 μM H_2folate. Column b shows data from DHFR burst experiments conducted in the presence of TS ligands FdUMP, and CH_2H_4folate. The conditions were used were 7.5 μM enzyme, 500 μM NADPH, 100 μM FdUMP, and 25 μM CH_2H_4folate, mixed with 50 μM H_2folate. WT data points are shown in red, Ala-FACE data points in blue, and D4 data points in green. In all cases, the data were fit to a single-exponential equation, and the rate constants from these are summarized in Table 2.

Table 2: Summary of DHFR Rate Constants from Stopped-Flow FRET Experiments under Burst Conditions[a]

	+no TS ligands	+FdUMP +CH_2H_4 folate
WT DHFR burst rate (s^{-1})	61.0 ± 7.52	135 ± 9.18
Ala-FACE DHFR burst rate (s^{-1})	68.0 ± 8.14	161 ± 7.09
D4 DHFR burst rate (s^{-1})	28.9 ± 4.56	63.2 ± 2.93

[a] The data were fit to a single-exponential burst equation, and the conditions used were as summarized in the legend for Figure 4.

at the TS active site. Second, the rates of the activated *P. falciparum* and *L. major* DHFRs are about 130 s^{-1} and 120 s^{-1} (*6*), respectively, while the rate constants of DHFR from *C. hominis* and *T. gondii* are about 130 s^{-1} and 180 s^{-1}, respectively. This suggests that these four parasitic TS-DHFR enzymes have similar in vitro DHFR chemical rates but different methods of activation. And third, since presumably the *P. falciparum* TS-DHFR is in a liganded state in the cell, this activated DHFR rate is probably a more accurate representation of the chemical rate. Our data also show that a reciprocal communication occurs between TS and DHFR in the WT enzyme, as the TS rate is activated in the presence of the DHFR ligand, NADPH.

This communication between active sites is likely mediated by conformational changes to the enzyme active site initiated by ligand binding, a well-studied phenomenon in both the *E. coli* TS and DHFR enzymes (*18*−*22*). In fact, when we performed the DHFR reactions in the presence of only FdUMP (without CH_2H_4folate), the DHFR chemical rates were not activated (data not shown). The published crystal structure of *P. falciparum* TS-DHFR has a doubly liganded DHFR active site [bound with NADPH and WR99210, a triazine DHFR inhibitor (*23*, *24*)] but only a singly liganded TS active site (bound with dUMP but no folate ligand) (*9*). It would be interesting to see if our kinetic data on activation and communication are reflected in significant structural differences in a TS-DHFR where the TS is doubly liganded. If the DHFR active site is conformationally different in the presence of a fully liganded TS, then these activation data could have considerable implications for structure-based drug design against *P. falciparum* TS-DHFR.

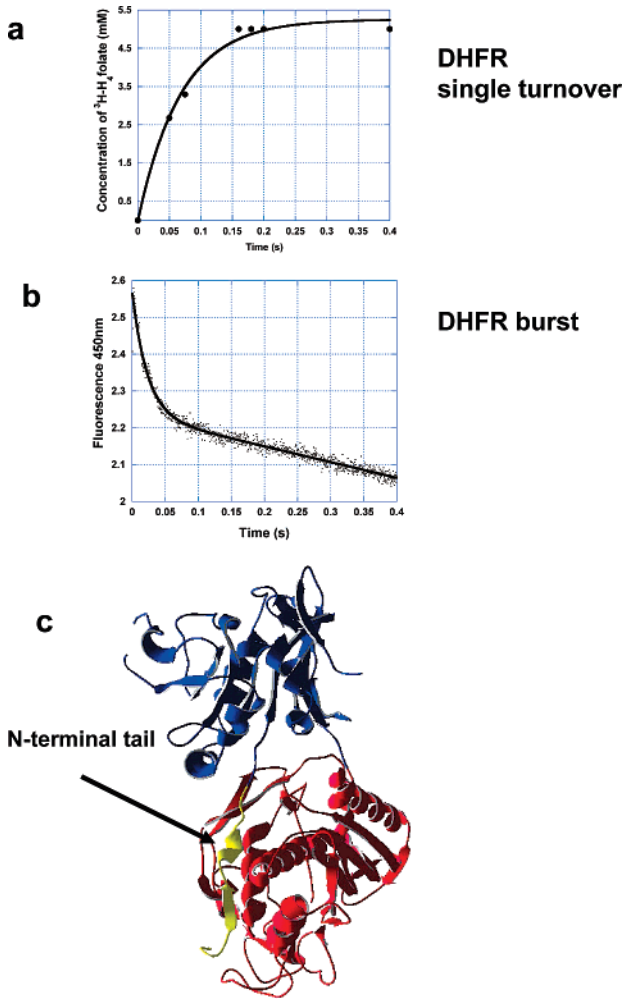

FIGURE 5: DHFR reactions of the *L. major* N-terminal deletion mutant N22 show that the N-terminal tail is autoinhibitory in the *L. major* TS-DHFR enzyme. (a) Single-turnover, rapid chemical quench experiments for N22 conducted with 45 μM enzyme and 500 μM NADPH mixed with 5.5 μM tritiated H_2folate. The data were fit to a single-exponential equation to provide a rate constant of 40.2 + 4.6 s^{-1}. In comparison, the DHFR single-turnover rate for WT *L. major* TS-DHFR had a rate constant of 14.5 ± 1.37 s^{-1} (data not shown). (b) N22 mutant DHFR burst experiment, performed in the stopped-flow apparatus, was conducted with 7.5 μM enzyme and 500 μM NADPH, mixed with 50 μM H_2folate. The fluorescence excitation was at 287 nm and the emission was at 450 nm. The data were fit to a single-exponential burst equation to provide a rate constant of 45.21 + 0.853 s^{-1}. (c) The *L. major* TS-DHFR structure is colored with DHFR domains in blue, TS in red, and the N-terminal tail in yellow; the N-terminal tail wraps around and makes extensive contacts with the TS domain. The substrates methotrexate, NADPH, FdUMP, and 10-propargyl-5,8-dideazafolate (PDDF) are shown in gray.

Crossover Helix Mutant of P. falciparum TS-DHFR Enzyme. Our results show that the crossover helix does not play a role in modulating catalysis in *P. falciparum* TS-DHFR. We designed several mutations of the crossover helix (residues 284−295) in the linker region of the *P. falciparum* TS-DHFR enzyme, and we probed these mutants for changes in the chemical rates of the TS, DHFR, and bifunctional TS-DHFR reactions. The sequence encoding the crossover helix has no homology to the linker region of other parasitic TS-DHFRs, but the helix itself is conserved in the *C. hominis* and *T. gondii* TS-DHFR enzymes. In *P. falciparum*, the crossover helix is very negatively charged and interacts with positively charged residues of the backside of the active site of DHFR (as shown in Figure 2b) (*9*). The importance of this helix, already suggested by its numerous interactions with the DHFR domain, was compounded by unpublished data from W. Sirawaraporn demonstrating that the shortest region of a linker−TS construct that could interact with DHFR started at residue 282, immediately N-terminal to the crossover helix. In *C. hominis*, mutations of the crossover helix have been shown to reduce DHFR activity (*11*).

Thus, we designed three mutations of the crossover helix: (1) deletion of the entire helix (Δ-helix), (2) substitution of all residues of the helix with alanines (all-Ala), and (3) substitution of only those residues on the face of the helix that interact with the backside of the DHFR active site (Ala-FACE). The Δ-helix and all-Ala mutations underwent significant intracellular proteolysis and could not be expressed in sufficient quantity for detailed kinetic analysis.

The Ala-FACE enzyme had TS, DHFR, and TS-DHFR chemical rates that were very similar to WT, under both single-turnover and pre-steady-state burst conditions (Tables 1 and 2). Also, the Ala-FACE enzyme had a similar activation of the DHFR chemical rate by TS ligands (Table 2) and of the TS rate by the DHFR ligand NADPH. Taken together, these results suggest that the crossover helix perhaps plays a role in stabilizing the interaction between TS and DHFR in the *P. falciparum* bifunctional enzyme but does not affect catalytic rate directly. Significant disruption of the electrostatic interactions of the helix, or deletion of the helix, might expose previously internalized regions of the enzyme to cytosolic proteases. Since disruption of crossover helix interactions in *C. hominis* significantly decreases the DHFR catalytic rate, similar results for the *P. falciparum* enzyme had initially been expected. However, in *P. falciparum*, the much higher prevalence of acidic residues in, and the larger number of electrostatic interactions made by, the helix with the DHFR backbone perhaps renders this crossover helix more critical in maintaining structural integrity in this large enzyme.

D4 N-Terminal Mutant of P. falciparum TS-DHFR Enzyme. The N-terminal tail of the *P, falciparum* protein comprises only residues 1−6, and yet two previous studies have suggested it plays an important role in DHFR activity and the interaction between TS and DHFR domains (*12*, *13*). Shallom et al. (*13*) demonstrated that the integrity of the N-terminal region of *P. falciparum* DHFR is essential for TS to be active. Wattanarangsan et al. (*12*) made sequential deletions of the N-terminal region of the DHFR domain and found that the number of amino acids deleted from the N-terminal tail corresponded with decreasing DHFR activity. They also suggest that TS will remain active in the presence of a conformationally intact DHFR, even though the DHFR enzyme has significantly impaired activity. One must note that neither of these previous studies was carried out on the full-length, bifunctional *P. falciparum* TS-DHFR enzyme or involved pre-steady-state kinetic analysis. They involved expressing monofunctional *P. falciparum* DHFR and linker−TS constructs and monitoring their interaction via complementation assays in *E. coli*.

Our results confirm that deleting the N-terminal tail in *P. falciparum* TS-DHFR decreases DHFR catalytic rate (Figures 3 and 4). Furthermore, our data newly suggest that the rate of the bifunctional TS-DHFR reaction is 2-fold slower in the D4 mutant than in WT, although the TS chemical rate

in the D4 mutant is about two-thirds that of WT (Table 2, Figure 3c). We also show that 2-fold activation of DHFR rate by TS ligands remains intact in the D4 mutant (Table 2) but is impaired in the activation of TS by the DHFR ligand NADPH.

It is imperative to note that the bifunctional D4 mutant is significantly more active than might have been suggested by the previous studies on the monofunctional DHFR (*12*). Wattanarangsan et al. (*12*) show the D4 DHFR mutant to be 80-fold less active than WT DHFR when activity is determined spectrophotometrically from crude extract and over 400-fold less active when DHFR activity is determined by bacterial complementation assay. In our studies, the D4 mutant DHFR rate is only 2-fold decreased compared to WT under single-turnover conditions and about 30-fold decreased under steady-state conditions. Also, we show that the full-length D4 mutant has impaired bifunctional TS-DHFR activity under both single-turnover and steady-state conditions (Figure 3b). We attribute the differences between the monofunctional and bifunctional D4 enzyme studies to the elegant communication between TS and DHFR domains in the intact enzyme. Our results also suggest that the DHFR ligand NADPH does not activate TS activity, which might explain why the bifunctional TS-DHFR chemical rate is somewhat slower than the TS single-turnover rate alone. The differences in our pre-steady-state in vitro data, compared to previous studies on N-terminal mutants, may also be accounted for by the different microenvironment of the intracellular environment.

Why does the N-terminal tail, although remote from the active site, affect catalysis? Since D4 DHFR can still be activated in the presence of TS ligands (Figure 4), and since substrate channeling from TS to DHFR domains remains unperturbed in the D4 mutant (data not shown), we suggest that the D4 mutant is affecting coordinated, domain−domain motions that occur during catalysis and ligand binding in DHFR. Such movements have been clearly demonstrated in *E. coli* DHFR (*18*, *22*) and TS enzymes (*19*−*21*). Close examination of the structure of *P. falciparum* TS-DHFR shows that the N-terminal tail is distant from the active site but can interact with helices in insert II (a 35 aa region unique to plasmodial DHFRs) and the $\alpha\beta$ loop, which encodes part of the active site (*9*) (Figure 2c). Thus, the interaction between these loops and the N-terminal tail may be essential in the coordinated motions of DHFR during catalysis. Since the structure of the fully liganded, *P. falciparum* TS-DHFR enzyme has not yet been solved, there may be additional, or distinct, interactions between the N-terminal tail and regions linked to the DHFR active site that are not fully appreciable with the present structure.

It should be noted, however, that our data cannot exclude solvation differences between WT and mutant enzymes to account for the difference in their activities. We would expect such differences to be negligible, given that only four amino acids were deleted to make the D4 mutant. However, such potential solvation differences may especially become important in ligand design if the N-terminal tail of *P. falciparum* TS-DFHR is targeted in rational drug design (*25*−*27*).

A comparison of mutant forms of the enzyme with WT requires normalization of the active functional protein. Our previous studies on other enzymes have established that using equivalent active-site concentrations in pre-steady-state burst experiments offers a reliable means for comparing WT and mutant bifunctional TS-DHFR proteins. The steady-state determination of TS specific activity has also been suggested as a reliable indicator of functional protein (*28*) but cannot be used to compare mutants with impaired TS function.

N22 N-Terminal Mutant of the L. major TS-DHFR Enzyme. We wanted to determine whether deleting the 22 aa N-terminal tail in *L. major* TS-DHFR would also decrease the DHFR catalytic rate. Surprisingly, we found that the N22 mutation had a faster single-turnover DHFR rate, an observation confirmed with pre-steady-state burst studies in the stopped-flow apparatus (Figure 5a,b). Since the N-terminal tail in *L. major* makes extensive contacts with the TS domain (Figure 5c) (*10*), perhaps it is playing an autoinhibitory role and is dislocated during the coordinated motions that accompany catalysis in TS and DHFR enzymes. The pre-steady-state DHFR burst experiment in the presence of TS ligands for the N22 mutant shows that the enzyme has lost its DHFR burst when TS is activated (data not shown), although it is already known that the WT *L. major* enzyme demonstrates clear domain−domain communication between DHFR and TS (*6*). Therefore, we conclude that deleting the *L. major* TS-DHFR N-terminal tail leads to a faster DHFR rate of chemistry and a disruption in the activation of DHFR by TS. Furthermore, the N-terminal tail plays opposite roles in *L. major* and *P. falciparum* TS-DHFRs. Perhaps because of the extensive contacts it makes with the TS domain, the N-terminal tail may play an autoinhibitory role, and must be dislocated for the enzyme to be active (Figure 5c).

Summary and Implications for Parasitic Bifunctional TS-DHFRs and Inhibitor Design. This is the first systematic, in-depth, pre-steady-state kinetic analysis of the nonactive-site regions of any bifunctional TS-DHFR enzyme, especially one from *P. falciparum*. Our results show that, in the WT enzyme, TS catalyzes the rate-limiting step, and communication occurs between the TS and the DHFR domains. Mutations to the face of the crossover helix in the linker region affect neither the rate of catalysis at either active site nor interdomain communication. Deletion of the N-terminal tail of *P. falciparum* TS-DHFR decreases the DHFR single-turnover rate by half and the bifunctional TS-DHFR rate by about a third. While the DHFR rate can still be activated 2-fold in the presence of TS ligands, reciprocal activation of TS by DHFR ligands is impaired in the D4 mutant. However, an analogous deletion in the N-terminal tail of the *L. major* TS-DHFR N-terminal tail leads to a 3-fold-activated DHFR rate and impaired DHFR-to-TS communication.

Even though there is overall structural similarity in parasite TS-DHFRs, general conclusions about enzyme mechanism cannot be drawn: TS-DHFR enzymes from different parasites are regulated very differently, and there is minimal kinetic basis for previous phylogenetic classification of these TS-DHFR enzymes by homologous structural features (*29*). The N-terminal tail can have both an activating and an autoinhibitory role. The crossover helix in the linker may increase catalytic activity or have a minimal effect on the rate of chemistry at DHFR (*7*). Each one of these enzymes is unique and elegant in its design. The impact of these nonactive mutations needs to be further elucidated in cell culture models of *P. falciparum* and *L. major* parasites. More studies are needed to dissect the interaction of the DHFR

N-terminal tail with its neighboring helices in the DHFR domain.

Implications for Novel Therapeutics. In many well-characterized enzymes like HIV reverse transcriptase and HIV-1 protease, the importance of nonactive-site regions in drug design and drug resistance is already well-appreciated (*30*, *31*). Even in human and *E. coli* DHFRs, the nonactive-site regions have long been known to play an important role in therapeutics and regulation of expression (*32*, *33*). Antifolates are used in the clinic for treatment of malaria and leishmaniasis, and in both cases, toxicity is a limiting factor in high-dose treatment (*34*). Thus, a better understanding of the nonactive-site regions, with no homologous counterparts in the corresponding human enzymes, could lead to the development of more targeted therapy. In *P. falciparum* TS-DHFR, inhibitors directed toward the N-terminus could be used in combination with active-site inhibitors for a synergistic inhibition of the malaria TS-DHFR. Our study, examining the functional contributions of nonactive-site regions in *P. falciparum* and *L. major* TS-DHFR, thus has implications in the design of novel, selective, less toxic therapies for these parasitic diseases.

ACKNOWLEDGMENT

We thank Dr. Melissa Vargo, Walter (Eddie) Martucci, and Dr. Lanxuan (Cindy) Doan for helpful discussions in the preparation of the manuscript.

REFERENCES

1. Greenwood, B. M., et al. (2005) Malaria, *Lancet 365* (9469), 1487−1498.
2. Ivanetich, K. M., and Santi, D. V. (1990) Thymidylate synthase-dihydrofolate reductase in protozoa, *Exp. Parasitol. 70* (3), 367−371.
3. Yuthavong, Y. (2002) Basis for antifolate action and resistance in malaria, *Microbes Infect. 4* (2), 175−182.
4. Ivanetich, K. M., and Santi, D. V. (1990) Bifunctional thymidylate synthase-dihydrofolate reductase in protozoa, *FASEB J. 4* (6), 1591−1597.
5. Atreya, C. E., and Anderson, K. S. (2004) Kinetic characterization of bifunctional thymidylate synthase-dihydrofolate reductase (TS-DHFR) from *Cryptosporidium hominis*: a paradigm shift for ts activity and channeling behavior, *J. Biol. Chem. 279* (18), 18314−18322.
6. Liang, P. H., and Anderson, K. S. (1998) Substrate channeling and domain−domain interactions in bifunctional thymidylate synthase−dihydrofolate reductase, *Biochemistry 37* (35), 12195−12205.
7. Doan, L. T., et al. (2007) Nonconserved Residues Ala287 and Ser290 of the *Cryptosporidium hominis* Thymidylate Synthase Domain Facilitate Its Rapid Rate of Catalysis, *Biochemistry 46* (28), 8379−83791.
8. O'Neil, R. H., et al. (2003) The crystal structure of dihydrofolate reductase-thymidylate synthase from Cryptosporidium hominis reveals a novel architecture for the bifunctional enzyme, *J. Eukaryot. Microbiol. 50* (Suppl.), 555−556.
9. Yuvaniyama, J., et al. (2003) Insights into antifolate resistance from malarial DHFR-TS structures, *Nat. Struct. Biol. 10* (5), 357−365.
10. Knighton, D. R., et al. (1994) Structure of and kinetic channelling in bifunctional dihydrofolate reductase-thymidylate synthase, *Nat. Struct. Biol. 1* (3), 186−194.
11. Vargo, M. A., and Anderson, K. S. (2008) Exploring interactions of the cross-over helix of *C. hominis* Thymidylate Synthase-Dihydrofolate Reductase, manuscript in preparation.
12. Wattanarangsan, J., et al. (2003) Effect of N-terminal truncation of *Plasmodium falciparum* dihydrofolate reductase on dihydrofolate reductase and thymidylate synthase activity, *Mol. Biochem. Parasitol. 126* (1), 97−102.
13. Shallom, S., et al. (1999) Essential protein-protein interactions between *Plasmodium falciparum* thymidylate synthase and dihydrofolate reductase domains, *J. Biol. Chem. 274* (53), 37781−37786.
14. Mathews, C. K., and Huennekens, F. M. (1960) Enzymic preparation of the 1,L-diastereoisomer of tetrahydrofolic acid, *J. Biol. Chem. 235*, 3304−3308.
15. Curthoys, N. P., Scott, J. M., and Rabinowitz, J. C. (1972) Folate coenzymes of *Clostridium acidi-urici*. The isolation of L-5,10-METHENYLTETRAHYDROPTEROYLTRIGLUTAMATE, ITS CONVERSION TO L-TETRAHYDROPTEROYLTRIGLUTAMATE AND L-10-[^{14}C]FORMYLTETRAHYDROPTEROYLTRIGLUTAMATE, AND THE SYNTHESIS OF L-10-FORMYL-[6,7-$^{3}H_2$]TETRAHYDROPTEROYLTRIGLUTAMATE AND L-[6,7-$^{3}H_2$]TETRAHYDROPTEROYLTRIGLUTAMATE, *J. Biol. Chem. 247* (7), 1959−1964.
16. Chitnumsub, P., et al. (2004) Characterization, crystallization and preliminary X-ray analysis of bifunctional dihydrofolate reductase-thymidylate synthase from *Plasmodium falciparum*, *Acta Crystallogr. D: Biol. Crystallogr. 60* (Pt. 4), 780−783.
17. Meek, T. D., Garvey, E. P., and Santi, D. V. (1985) Purification and characterization of the bifunctional thymidylate synthetase-dihydrofolate reductase from methotrexate-resistant *Leishmania tropica*, *Biochemistry 24* (3), 678−686.
18. Rod, T. H., Radkiewicz, J. L., and Brooks, C. L., 3rd. (2003) Correlated motion and the effect of distal mutations in dihydrofolate reductase. *Proc. Natl. Acad. Sci. U.S.A. 100* (12), 6980−6985.
19. Schnell, J. R., Dyson, H. J., and Wright, P. E. (2004) Structure, dynamics, and catalytic function of dihydrofolate reductase, *Annu. Rev. Biophys. Biomol. Struct. 33*, 119−140.
20. Stroud, R. M., and Finer-Moore, J. S. (1994) Stereochemistry of a multistep/bipartite methyl transfer reaction: thymidylate synthase, *FASEB J. 7* (8), 671−677.
21. Matthews, D. A., et al. (1920) Stereochemical mechanism of action for thymidylate synthase based on the X-ray structure of the covalent inhibitory ternary complex with 5-fluoro-2′-deoxyuridylate and 5,10-methylenetetrahydrofolate, *J Mol Biol 214* (4), 937−948.
22. McElheny, D., et al. (2005) Defining the role of active-site loop fluctuations in dihydrofolate reductase catalysis, *Proc. Natl. Acad. Sci. U.S.A. 102* (14), 5032−5037.
23. Edstein, M. D., et al. (1997) In vitro activities of the biguanide PS-15 and its metabolite, WR99210, against cycloguanil-resistant *Plasmodium falciparum* isolates from Thailand, *Antimicrob. Agents Chemother. 41* (10), 2300−2301.
24. Canfield, C. J., et al. (1993) PS-15: a potent, orally active antimalarial from a new class of folic acid antagonists, *Am. J. Trop. Med. Hyg. 49* (1), 121−126.
25. Lafont, V., et al. (2007) Compensating enthalpic and entropic changes hinder binding affinity optimization, *Chem.-Biol. Drug Des. 69* (6), 413−422.
26. Rodriguez-Larrea, D., et al. (2006) Role of solvation barriers in protein kinetic stability, *J. Mol. Biol. 360* (3), 715−724.
27. Whitesides, G. M., and Krishnamurthy, V. M. (2005) Designing ligands to bind proteins. *Q. Rev. Biophys. 38* (4), 385−395.
28. Mudeppa, D. G., et al. (2007) Cell-free production of functional *Plasmodium falciparum* dihydrofolate reductase-thymidylate synthase, *Mol. Biochem. Parasitol. 151* (2), 216−219.
29. O'Neil, R. H., et al. (2003) Phylogenetic classification of protozoa based on the structure of the linker domain in the bifunctional enzyme, dihydrofolate reductase-thymidylate synthase, *J. Biol. Chem. 278* (52), 52980−52987.
30. Olsen, D. B., et al. (1999) Non-active site changes elicit broad-based cross-resistance of the HIV-1 protease to inhibitors, *J. Biol. Chem. 274* (34), 23699−23701.
31. Muzammil, S., Ross, P., and Freire, E. (2003) A major role for a set of non-active site mutations in the development of HIV-1 protease drug resistance, *Biochemistry 42* (3), 631−638.
32. Dicker, A. P., et al. (1993) Methotrexate resistance in an in vivo mouse tumor due to a non-active-site dihydrofolate reductase mutation, *Proc. Natl. Acad. Sci. U.S.A. 90* (24), 11797−11801.
33. Skacel, N., et al. (2005) Identification of amino acids required for the functional up-regulation of human dihydrofolate reductase protein in response to antifolate treatment, *J. Biol. Chem. 280* (24), 22721−22731.
34. Sands, M., Kron, M. A., and Brown, R. B. (1985) Pentamidine: a review, *Rev. Infect. Dis. 7* (5), 625−634.

BI701624U